A Geochemical and Geophysical Examination of Submarine Groundwater Discharge and Associated Nutrient Loading Estimates into Lynch Cove, Hood Canal, WA

Peter W. Swarzenski[*1], *F. William Simonds*[2], *Tony Paulson*[2], *Sarah Kruse*[3] *and Chris Reich*[1]

[1]U.S. Geological Survey, 600 4th Street South, St. Petersburg, FL 33701

[2]U.S. Geological Survey, 934 Broadway, Suite 300, Tacoma, WA 98402

[3]Department of Geology, University of South Florida, Tampa, FL 33620

* Corresponding author phone: 727-803-8747 x. 3072; fax: 727-803-2032; email: pswarzen@usgs.gov

ABSTRACT

Geochemical tracer data (i.e., ^{222}Rn and four naturally occurring Ra isotopes), electromagnetic (EM) seepage meter results, and high-resolution, stationary electrical resistivity images are used to examine the bi-directional (i.e., submarine groundwater *discharge* and *recharge*) exchange of a coastal aquifer with sea water. Our study site for these experiments was Lynch Cove, the terminus of Hood Canal, WA, where fjord-like conditions dramatically limit water column circulation that can lead to recurring summer-time hypoxic events. In such a system a precise nutrient budget may be particularly sensitive to groundwater-derived nutrient loading. Shore-perpendicular time-series subsurface resistivity profiles show clear, decimeter-scale tidal modulation of the coastal aquifer in response to large, regional hydraulic gradients, hydrologically-transmissive glacial terrain, and large (4-5m) tidal amplitudes. A 5-day ^{222}Rn time-series shows a strong inverse covariance between ^{222}Rn activities (5 - 30 dpm L^{-1}) and water level fluctuations, and provides compelling evidence for tidally-modulated exchange of groundwater across the sediment / water interface in this system. Mean Rn-derived submarine groundwater discharge (SGD) rates of 85±84 cm d^{-1} agree closely in the timing and magnitude with EM seepage meter results that showed discharge (up to 80 cm d^{-1}) during low tide and recharge during the high tide events. To evaluate the importance of fresh *versus* saline SGD, Rn-derived SGD rates (as a proxy of total SGD) are compared to excess ^{226}Ra-derived SGD rates (as a proxy for the saline contribution of SGD). The calculated SGD rates, which include a significant (>80%) component of recycled sea water, are used to estimate associated nutrient (NH_4^+, Si, PO_4^{-3}, NO_3+NO_2, TDN) loads to Lynch Cove. The dissolved inorganic nitrogen (DIN = NH_4+NO_2+NO_3) SGD loading estimate of 5.9 x 10^4 mol d^{-1} is

one to two orders of magnitude larger than similar estimates derived from atmospheric deposition and surface water runoff, respectively.

Keywords: submarine ground water discharge, radon, radium, multi-electrode stationary DC resistivity

Introduction

Research on coastal aquifer dynamics, which may include both submarine groundwater *discharge* (SGD) and *recharge* processes, has surged over the past decade as coastal scientists, armed with new tools and geochemical tracers have been able to identify and quantify the importance of SGD to varied coastal material and water budgets (1-7). The discharge of nutrient-enriched groundwater into coastal waters contributes towards nutrient enrichments that may lead to phytoplankton blooms (8-11), eutrophication (12-13), and general ecosystem deterioration (14). Discharge of coastal groundwater most often is diffuse and ephemeral, rather than via distinct, submarine vent features (15), making accurate assessments of SGD rates particularly difficult. New geochemical tracer techniques (16-20) and multi-electrode direct-current (DC) geophysical methods (21) have consequently been developed to better constrain SGD rates, forcing factors, scales, and potential ecological impacts.

Submarine groundwater discharge (SGD) has been defined to include the bi-directional exchange of any water mass across the sediment / water interface, regardless of its origin, composition, or driving force (5). Because the composition of this dynamic water mass can span a broad salinity gradient, a geochemical tracer used as a proxy to derive such SGD flux rates should ideally not be affected by changing salinity regimes, or at least should respond to such shifts in salinity predictably and consistently. From previous work, we now know that while Rn appears to be an effective tracer of total (fresh + saline) groundwater discharge (6, 22-24), Ra isotopes typically track mostly the saline contribution (3-4, 7, 9, 19, 25). The utility of a combined Ra/Rn study would thus yield information of the various components of groundwater discharge (26-27). Quantification of SGD rates

using either Ra or Rn rely on simple mass balance equations, where inputs and loss terms are quantified to yield excess flux rates (dpm m^{-2} hr^{-1}) that are then divided by a representative groundwater concentration (7, 17).

Electrical resistivity is ideally suited to coastal groundwater studies, as subtle shifts in the fresh water / salt water interface can be readily visualized using standard inversion routines (28). New multi-electrode cable configurations routed through multi-channel receivers enable much more detailed and rapid data acquisition. Using such a cable in stationary mode, time-series results yield new information on the forcing factors that control the position and dynamics of the fresh water / salt water interface (21).

Our study site is situated along Lynch Cove, which forms the terminus of Hood Canal, a 110km long, narrow (2-4km), deep (up to 175m) fjord-like estuary of Puget Sound (Figure 1). In Lynch Cove, in spite of a large (~4-5m) tidal range, circulation is greatly restricted, and as a consequence, dissolved oxygen concentrations in the water column are sometimes low enough to cause summer-time hypoxic events and associated fish stresses. The objective of this work is to evaluate and quantify the role of submarine groundwater discharge in the delivery of nutrients to this coastal system. Results suggest that both submarine groundwater discharge and recharge are overwhelmingly tidally modulated, and measured localized flux rates in excess of 80 cm d^{-1} yield significant associated nutrient loading estimates that warrant refinements to existing nutrient budgets.

Methods

Field work was conducted during June 6-12, 2006. While additional geochemical and geophysical data were collected at other sites along Lynch Cove, here we present results

only of a time-series experiment where simultaneous electromagnetic (EM) seepage meter, ^{222}Rn, and stationary multi-electrode resistivity results were collected at the same site ('Merrimont') (Figure 1). Time-series surface water and groundwater samples from 185cm depth using a drive point piezometer were also collected (Table 1) at the same site for a suite of nutrients (NH_4^+, Si, PO_4^{-3}, DIN, DON, and TDN). Nutrient analyses were conducted at Woods Hole Oceanographic Institute using standard colormetric techniques (4, 26). The activities of all four Ra isotopes were determined in groundwater and surface water collected at the Merrimont site, as well as from 5 stations (HC1-5) along the axis of Hood Canal/Lynch Cove and from the Skokomish River (Figure 1; Table 2). Briefly, 75-100L of surface water and 20L of groundwater were slowly filtered (~1L min^{-1}) through Mn-impregnated fiber columns and the fiber was subsequently analyzed first for ^{223,224}Ra using delayed coincidence counters, and then a high resolution gamma well detector was used for the two long-lived ^{226,228}Ra isotopes, as per methods of Moore and Arnold (29), Moore (3, 19), and Swarzenski et al. (15, 26-27). Expected error for the two short-lived and the two long lived Ra isotopes is ~10% and ~7%, respectively.

Multi-electrode Resistivity and Electromagnetic Seepage Meters. For stationary DC resistivity (resistivity = electrical conductivity^{-1}) surveys, an Advanced Geosciences Inc. (AGI) SuperSting eight-channel receiver was interfaced to a 56 electrode 112m cable (2m electrode spacing) through an external switching box. In this configuration, current potentials are measured in a distributed dipole-dipole array to maximize resolution and the signal-to-noise ratio, while minimizing data acquisition time (21). Resistivity values were processed with AGI's 2D EarthImager software using a homogenous starting model and a water depth measured at the mid-point of the survey. To force the inversion to emphasize

the fit of readings sampling the very near-shore environment, shallow readings from the seaward end of the line were excluded from the inversion procedure. Excluded readings were those whose position on the AGI pseudosection plot for dipole-dipole geometries lay above and seaward of a line extending from 56 meters along the profile at zero depth to 80 meters at 13 meters depth. Note that only the most landward 40m of each profile are shown in Figure 2A-E. Water column resistivities were allowed to float, as fixing the water column resistivity to an incorrect value can lead to significant errors in the inversion (30). Inversion parameters were set to AGI's default values for smooth inversion with the following exceptions: the criteria for removal for low-value resistivity data was 0.001 ohm-m; the stabilizing and damping factors were set to 100; the horizontal/vertical roughness ratio to 0.2, the resolution factor to 0, and the minimum allowed resistivity to 0.01 ohm-m.

An autonomous electromagnetic (EM) seepage meter, which consists of a 2.54cm ID EM flow meter attached directly to a 100cm-diameter dome-shaped housing (31), was also equipped with two Solinist conductivity, pressure and temperature sensors mounted inside and on top of the dome. A daily flux rate of 20cm would require 24 hours to replace the volume of water within the seepage meter. This seepage meter records a bi-directional flow rate reading every minute and stores the data in an internal data memory card.

Time Series Radon. In spite of its well-known effectiveness as a proxy of fluid exchange across the sediment / water interface (32), only recent advances (20, 23-24, 33) in how one can determine ^{222}Rn ($t_{1/2}$ = 3.82 days) accurately and quickly in the field have allowed a much greater number of data points to be collected and also interpreted. This 'field' analytical method is based on a simple premise that by knowing the temperature

dependent air-water partitioning coefficient of Rn, one can determine the concentration of Rn in water by measuring the equilibrated concentration in air using a commercially available (Durridge, Inc.) air Rn monitor. The equilibration process is accomplished in a simple exchanger where a stream of sea water is diffused through a constrictive nozzle.

At Lynch Cove, we measured the near-continuous ^{222}Rn concentration in the water column during a 5-day time series from the seaward end of a floating dock using a submersible pump positioned at a fixed distance (~15cm) above the seafloor. Concurrent with the Rn analyses, a continuous record of the temperature, salinity, and depth of the water column was collected using a calibrated YSI multi-parameter probe.

Results and Discussion

Stationary Resistivity. Resistivity results reported here are semi-quantitative 'snap-shots' of the dramatic response of fresh water / salt water interface of the coastal aquifer to tidal fluctuations. The steep bathymetric gradients and large tidal range observed at the Merrimont site required that post-processing routines incorporated both water column salinity and bathymetry. Figure 2 shows a time series of the resistivity in relation to tidal variability along a shore-perpendicular 112m long transect, where electrode 1 was positioned most landward and electrode 56 was located most seaward in ~15-20m of water. To address in detail processes at the land / sea boundary, only the first 40m of each image are shown. Each of the five images (A-E) was collected and processed identically; thus the change in resistivity along each time step can be discussed in terms of forcing factors, without the complication of a changing hydrogeologic framework or variable water column.

During high tide (Figure 2A), when the water line was located between electrode 5 and 6, the modeled resistivities were lowest (3-10 Ohm-m), implying that a freshened groundwater plume was least developed. From a suite of forward modeling experiments, we note that the lower limit (~20m) of the freshened water mass is rather poorly constrained. However, the freshened water plume to 20m depth is constrained by the data. With a falling tide, one can observe the lateral migration of a freshened groundwater plume towards Lynch Cove. At low tide (Figure 2D), the expression of the plume can be seen well past 30m and to depths >20m. A zone of high resistivity is consistently seen just landward of the waterline where numerous seeps (see Table 1) also developed at low tide. The expression of this water lens ('fresh water tunneling') is characteristic of density-driven recirculation combined with large fresh water heads and tidal fluctuations (34).

Time Series Radon. To evaluate the total (fresh + marine) contribution of submarine groundwater discharge to Lynch Cove, a 5-day time series of water column ^{222}Rn activities is used to calculate the advective flux rates. The premise of such calculations relies on an accurate mass balance of ^{222}Rn losses and gains over time and on a reasonable groundwater ^{222}Rn endmember concentration (35). Figure 3A shows the time series ^{222}Rn activities as a function of water depth; there is clear tidal modulation of groundwater-borne radon into the water column - at every low tide event a pronounced spike in the ^{222}Rn concentration was observed in spite of the large (4-5m) tidal range. To correct for supported radon in the water column, a mean ^{226}Ra activity of 5 dpm 100L^{-1} measured in surface waters at the Merrimont dock (Table 2) was subtracted from the ^{222}Rn values. For the 5-day time series, water column ^{222}Rn activities ranged from 0.5 to 29.0 dpm L^{-1}, with a mean of 4.9±3.7 dpm L^{-1} (n=729).

Applying a mass balance approach as per methods of Burnett and Dulaiova (6, 23), a calculated net ^{222}Rn flux rate ranged from – 24,700 to 25,400 dpm m^{-2} hr^{-1}, while a mixing-loss corrected total flux ranged up to 29,500 dpm m^{-2} hr^{-1}, depending on the tide. One can estimate groundwater discharge rates by dividing these flux rates by the radon concentration in representative discharging groundwater. A mean groundwater ^{222}Rn concentration (142 dpm L^{-1}) used to represent the discharging groundwater was derived from three piezometer (185cm depth) samples (^{222}Rn = 158±11, 129±25, and 140±35 dpm L^{-1}), which were also collected close to the landward end of Merrimont dock under fluctuating tides (Table 2). It is notable that groundwater ^{222}Rn activities changed little under different tidal regimes and was on the same order of magnitude as ^{222}Rn measured in nearby Merrimont spring (274±21 dpm L^{-1}). Using the calculated total flux rates results in a mean groundwater discharge rate of 85.8±84.5 cm d^{-1} (n=501). The large standard deviations reflect the dynamic mixing imposed by the large tidal range much more so than variable atmospheric evasion terms that peaked at just 1700 dpm m^{-2} hr^{-1} (mean = 210 dpm m^{-2} hr^{-1}, n=495).

EM Seepage Meter and bottom water conductivity. Figure 3B shows EM seepage meter results during the same 5-day time series. As for radon, the coincidence in the seepage rate peaks with low tide events illustrates clear tidal modulation of bi-directional SGD advection. As tidal fluctuations became larger later during the time series (note that the tidal range increased by almost 2m), so do observed seepage rates. If we more closely examine seepage meter results during the last tidal cycle where we have an uninterrupted, clean record, we not only see clear discharge events (up to 81 cm d^{-1}) that occur precisely at low tide but we also observe significant recharge or entrainment of coastal water into the

sediment during high tide events. The patterns of recharge very closely coincide with water level fluctuations, indicting that these processes are strongly modulated by the tides. While it is likely sheer coincidence that the EM seepage meter results yield a maximum rate so close to the Rn-derived estimate, the 5-day profile demonstrates the tidal control on groundwater discharge and recharge.

A conductivity profile (Figure 3C) collected by a Solinist Diver mounted on top of the seepage meter dome sampling bottom water shows a dramatic decrease (<34 mS cm^{-1}; salinity = 27.1) from a mean value of 40.7 mS cm^{-1} (n=241; salinity = 33.3) in conductivity at low tide during this last tidal cycle, a signal that was less clear earlier in the time series. It is likely that the conductivity (salinity) of the bottom waters at the Merrimont site reflect both an integrated signal that responds most directly to SGD after some critical threshold in advective rates or water level change is reached, and from the periodic seaward transport of fresher water in Lynch Cove. Note that the tidal range (Figure 3A) increased considerably along the time series. A separate record of conductivity from inside the seepage meter housing does not show a comparable decline in conductivity at low tide, suggesting that the placement of the meter was not directly on top of an active discharge site. Nonetheless, the pronounced decline in conductivity precisely at low tide and where both ^{222}Rn and the EM seepmeter data show clear surges confirms tidal modulation of groundwater / surface exchange at this site.

SGD Rates and Nutrient Loading. Scaling such SGD results up to reflect a realistic groundwater discharge rate per water body area and per unit time is a difficult but useful exercise to refine water budget calculations and material loading estimates. Shore-perpendicular, stationary resistivity profiles across the shore face at the Merrimont site can

yield important information as to the lateral and horizontal extent of the groundwater discharge / recharge zone. From Figure 2, it is evident that the coastal aquifer responds up to ~35m laterally and at least 20m vertically to tidally-driven water level fluctuations. Based on both hardware and software limitations, it is reasonable to expect that our resistivity images likely underestimate the total vertical and horizontal SGD scales. As these pulses in the coastal aquifer occur over a 9-hour cycle, a corresponding lateral exchange rate, assuming a mean sediment porosity of ~0.4, would be at least two orders of magnitude greater (~37 m d^{-1}) than the calculated Rn-derived upward SGD flux rate. While such calculations are first order estimates that describe the dynamic interplay of the coastal aquifer to tidal forcing, they do provide a sense of scale. For example, from the stationary resistivity data collected at the Merrimont site one can infer that the 4-5m tidal range can affect the fresh water / salt water interface of the coastal aquifer to depths of ~20m (80% of the local maximum water depth of Lynch Cove). One can accordingly adjust the total Lynch Cove area (2.89×10^6 m^2) to include only a perimeter ribbon where most tidally controlled SGD is expected to occur.

Alternatively, one can independently verify SGD scales by examining excess ^{226}Ra flux-derived SGD rates per entire Lynch Cove and by comparing such rates to Rn- or EM seepage meter-derived fluxes that define a more local SGD signal. For such calculations, a mean apparent residence time of 32 days (range for Lynch Cove = 25-40 days) is calculated using $^{223}Ra/^{228}Ra$ isotope ratios, as per methods of Moore (2-3) and utilized by Charette et al. (4) and Swarzenski et al. (26-27). This range is consistent with the findings of Paulson et al. (37). These authors reported that on September 22, 2004, the tip of an intrusion of warm, salty water passed the entrance of Lynch Cove and by October 25, 2004 the entire

Lynch Cove had a similar temperature-salinity signature. For the Ra-based residence time approach, we assume that the plume of surface water impacted by SGD will become isolated from bottom sediments so that radioactive decay processes alone can be used as water mass proxies. Such an assumption is validated by the occurrence of a persistent thermocline in Lynch Cove and Hood Canal, which deepened from 2m on June 2, 2006 to about 7m on June 9 that effectively separates bottom water from surface water (36). Excess ^{226}Ra fluxes (1.7×10^{7} dpm d^{-1}) are derived by subtracting the ^{226}Ra activity at HC1 from a mean Lynch Cove ^{226}Ra activity (4.2 dpm $100L^{-1}$), and then adjusting per volume (4.0×10^{8} m^3) and the computed residence time. Here we assume that the endmember HC1 sample reflects sea water most removed from Lynch Cove wherein Ra isotopes are effectively at background activities. Note that at HC1 and even HC2 no detectable ^{223}Ra was measured. We also ignore the influence of rivers in a mass balance of Ra in this system; Table 2 shows that the Ra activity in the Skokomish River is much lower than in Lynch Cove proper. As in the Rn model, a SGD rate per entire water body can be derived by dividing a mean ^{226}Ra groundwater value (5.0 dpm $100L^{-1}$; Table 2) from the excess Ra flux rates. Using this approach yields an SGD rate of 24 m^3 sec^{-1}, which amounts to an integrated vertical flux of 7.6 cm d^{-1}, assuming an area of 2.7×10^{7} m^2. It is acknowledged that this Ra approach represents a best estimate of saline SGD for the time period studied; more detailed information to better constrain endmember variability and seasonality would of course better refine these estimates.

Coastal nutrient budgets, particularly in enclosed water bodies with poor circulation, are sensitive to variable nutrient loading. Lynch Cove is uniquely poised to significant SGD influences as regional hydraulic gradients are favorable for coastal groundwater discharge,

the glacial coastal sediments are generally conducive to fluid transport, there are no large (i.e., $Q > 3\ m^3\ s^{-1}$) river inputs (i.e., the Skokomish and Tahuya Rivers discharge into Hood Canal proper, not Lynch Cove) to obscure SGD results, and the perimeter residential septic systems provide a potential source of groundwater-borne nutrients.

A recent study of dissolved inorganic nitrogen (DIN = NH_4+NO_2+NO_3) loading to Lynch Cove showed that while surface runoff and contributions from seasonal septic systems contribute about 25% and 23% of the DIN loads to the upper water column, respectively, about half of the total DIN load had a groundwater source (37). Paulson et al. (37) further divided the shoreline of Hood Canal and Lynch Cove into separate watershed sub-basins and developed respective DIN loading estimates per sub-basin. From their work, it is evident that the Merrimont site represents a shoreline typology with one of the largest groundwater discharge zones within the Lynch Cove area of Hood Canal and places the Rn- and EM-seepage meter-derived SGD rates observed at Merrimont into a regional context.

Nutrient (NH_4^+, Si, PO_4^{-3}, NO_2+NO_3, DIN, DON, and TDN) concentrations in groundwater and surface water collected during an ~9-hour time series at the Merrimont site and a low-tide seep water sample are shown in Table 1. The seep water sample (salinity = 4.6) has the highest observed Si (170 μM) and PO_4^{-3} (4.3 μM) concentration while the total dissolved nitrogen (TDN) concentration (14.6 μM) falls between respective mean groundwater (29.4 μM) and surface water (11.8 μM) values. Reduced N as NH_4^+ was not observed in the groundwater samples and only slightly (mean concentration = 0.7 μM) in the surface waters. The absence of NH_4^+ in coastal groundwater provides an additional line of evidence for the rapid transport/energetic mixing of the local coastal

aquifer with sea water. Silica was observed in groundwater at about 2 times the mean surface water concentration (70.7 μM), while the mean PO_4^{-3} concentration varied little in either sample set. Mean dissolved inorganic nitrogen (DIN) concentrations in groundwater and surface water samples are 24.2 μM and 1.5 μM, respectively, and on average make up about 82% and 13% of the groundwater and surface water total dissolved nitrogen (TDN) pool. The mean percentage of dissolved organic nitrogen (DON) in TDN in groundwater is 18% while in surface waters a mean of this ratio increased to 87%. Such high DON observed in surface waters may be, in part, the result of N fixing bacteria (38-39) or a signal from adjacent septic systems. While typically DIN has a more immediate and direct anthropogenic fingerprint, DON can be persistently bio-available for some time after N assimilation and mineralization (40). Figure 5 shows the molar distribution of PO_4^{-3} versus DIN. During our sampling, almost all the groundwater samples fall slightly below the Redfield 16:1 reference line, while all surface water samples are positioned well above this line. This depletion of inorganic N over PO_4^{-3} in surface water is indicative of a typical N-limited coastal system. However, as the mean molar DIN/PO_4^{-3} ratio (Figure 5A) for groundwater is so much larger than for similar surface water (1.2) or seep water (1.6) ratios, SGD loading of all N species is likely an important component of the nutrient budget.

Table 3 compares the calculated Rn- and Ra-derived SGD nutrient loading estimates to Lynch Cove using 1) mean groundwater (first and second rows) and 2) the low tide seep water nutrient concentrations (third row) of Table 1. A calculated ratio of the Ra- to Rn-derived SGD rate of 86% implies that the saline contribution of total SGD is large in this system, in spite of the large hydraulic heads, as evidenced, for example, in the downward

trending bottom water conductivity or artesian springs observed at low tide. If we accept that such SGD-derived nutrient loads are reasonable attempts at developing groundwater loading estimates that include a significant component of recycled sea water, then we can compare our results with other literature values. In all instances, the Ra-derived (i.e., saline SGD) nutrient loading estimates comprise ~83-86% of the respective Rn-derived (i.e., total SGD) loading estimates. This would imply that the fresh water SGD contribution alone would comprise ~14-17% of the total loads of the first four rows and the entire mass balance load in the fifth row (fresh groundwater) reported in Table 3. Using the low-tide seep water nutrient concentrations results in TDN and DIN loads that are ~50% and 30% lower, respectively, while DON remains similar in magnitude to loads calculated using mean groundwater nutrient concentrations. The calculated DIN loading estimates to Lynch Cove range about one order of magnitude from a high of 5.9×10^4 mol d^{-1} derived using the time-series ^{222}Rn (fresh + saline) SGD flux rate to 4.2×10^3 mol d^{-1} that was estimated by mass balance (37) of fresh water groundwater. Such agreement is encouraging, given the vastly different methodologies and sampling scales. When such results are compared to other nutrient mass balance components for Lynch Cove (37), such as atmospheric deposition (DIN = 3.3×10^2 mol d^{-1}) and surface water runoff (DIN = 2.1×10^3 mol d^{-1}), the role of SGD (fresh water and recycled sea water) in nutrient loading estimates to Lynch Cove becomes apparent. At the Merrimont site, time-series resistivity images across a shore-face show decimeter-scale oscillations of the fresh water / salt water interface in response to tidally-driven water level fluctuations. It is evident that most of the resistivity change occurs close to the moving water line and is strongly modulated by a large tidal range. From the resistivity and seepage meter data, both recharge as well as discharge

processes are important in material and water transport. The scales and dynamic nature of this coastal exchange can play an important role in the delivery and loading of fresh water or marine nutrients to Lynch Cove.

Acknowledgements

This work was conducted with supplemental support from the USGS Washington Science Center and from the USGS Puget Sound science team. PWS recognizes the continued financial support from the USGS Coastal & Marine Geology (CMG) Program and kindly thanks Dr. William Portuese for access to his home/dock along Lynch Cove. Additional expert field support was provided by Bob Rosenberry. Constructive reviews by W.S. Burnett, xx, and xx significantly improved this manuscript. The use of trade names is for descriptive purposes only and does not imply endorsement by the U.S. Government.

References

(1) Moore, W.S. Large groundwater inputs to coastal waters revealed by ^{226}Ra enrichment. *Nature* **1996**, 380, 612-614.

(2) Moore, W.S. The subterranean estuary: A reaction zone of groundwater and sea water. *Mar. Chem.* **1999**, 65, 111–125.

(3) Moore, W.S. Determining coastal mixing rates using radium isotopes *Cont. Shelf Res.* **2000**, 20, 1993-2007.

(4) Charette, M.A.; Buesseler, K.O.; Andrews, J.E. Utility of radium isotopes for evaluating the input and transport of groundwater-derived nitrogen to a Cape Cod estuary. *Limnol. Oceanogr.* **2001**, 46, 465-470.

(5) Burnett, W.C.; Bokuniewicz, H.; Huettel, M.; Moore, W.S.; Taniguchi, M. Groundwater and porewater inputs to the coastal zone. *Biogeochemistry* **2003a**, 66, 3-33.

(6) Burnett, W.C.; Dulaiova, H. Radon as a tracer of submarine groundwater discharge into a boat basin in Donnalucata, Sicily. *Cont. Shelf Res.* **2006**, 26, 862-873.

(7) Swarzenski, P.W. U/Th series radionuclides as tracers of coastal groundwater. *Chem. Rev.* **2007**, 107, 663-674, DOI: 10.1021/cr0503761.

(8) LaRoche, J.; Nuzzi, R.; Waters, R.; Wyman, K.; Falkowski, P.G.; Wallace, D.W.R. Brown tide blooms in Long Island's coastal waters linked to inter-annual variability in groundwater flow. *Global Change Biology* **1997**, 3, 397-410.

(9) Hwang, D.-W.; Kim, G.; Lee, Y.-W.; Yang, H.-S. Estimating submarine inputs of groundwater and nutrients to a coastal bay using radium isotopes. *Marine Chemistry* **2005**, 96, 61-71.

(10) Gobler, C.J.; Sanudo-Wilhelmy, S.A. Temporal variability of groundwater seepage and brown tide blooms in a Long Island embayment. *Mar. Ecol. Prog. Ser.* **2001**, 217, 299-309.

(11) Hu, C.; Muller-Karger, F.; Swarzenski, P.W. Hurricanes, submarine ground-water discharge and west Florida's red tides. *Geophys. Res. Lett.* **2006**, 33, L11601, doi:10.1029/2005GL025449.

(12) Capone, D.G.; Bautista, M.F. A groundwater source of nitrate in nearshore marine sediments. *Nature* **1985**, 313, 214-216.

(13) Giblin, A.; Gaines, A. Nitrogen inputs to a marine embayment: The importance of groundwater. *Biogeochemistry* **1990**, 10, 309–328.

(14) Johannes, R. The ecological significance of the submarine discharge of groundwater. *Mar. Ecol. Prog. Ser.* **1980**, 3, 365–373.

(15) Swarzenski, P.W.; Reich, C.D.; Spechler, R.M.; Kindinger, J.L.; Moore, W.S. Using multiple geochemical tracers to characterize the hydrogeology of the submarine spring off Crescent Beach, Florida. *Chem. Geol.* **2001**, 179, 187-202.

(16) Burnett, W.C.; Chanton, J.; Christoff, J.; Kontar, E.; Krupa, S.; Lambert, M.; Moore, W.; O'Rourke, D.; Paulsen, R.; Smith, C.; Smith, L.; Taniguchi, M.

Assessing methodologies for measuring groundwater discharge to the ocean. *EOS* **2002**, 83, 117-123.

(17) Burnett, W.C.; Cable, J.E.; Corbett, D.R. Radon tracing of submarine groundwater discharge in coastal environments. In *Land and Marine Hydrogeology;* Taniguchi, M.; Wang, K.; Gamo. T., Eds; Elsevier; 2003b; pp 25-43.

(18) Moore, W.S. High fluxes of radium and barium from the mouth of the Ganges-Brahmaputra River during low river discharge suggest a large groundwater source. *Earth Planet. Sci. Lett.* **1997**, 150, 141-150.

(19) Moore W.S. Sources and fluxes of submarine groundwater discharge delineated by radium isotopes. *Biogeochemistry* **2003**, 66, 75-93.

(20) Povinec, P.P.; Aggarwal, P.K.; Aureli, A.; Burnett, W.C.; Kontar, E.A.; Kulkarni, K.M.; Moore, W.S.; Rajar, R.; Taniguchi, M.; Comanducci, J.-F.; Cusimano, G.; Dulaiova, H.; Gatto, L.; Groening, M.; Hauser, S.; Levy-Palomo, I.; Oregioni, B.; Ozorovich, Y.R.; Privitera, A.M.G.; Schiavo, M.A. Characterization of submarine groundwater discharge offshore south-eastern Sicily. *J. Environ. Radioact.* **2006**, 89, 81-101.

(21) Swarzenski, P.W.; Burnett, W.C.; Greenwood, W.J.; Herut,B.; Peterson, R.; Dimova, N.; Shalem, Y.; Yechieli, Y.; Weinstein, Y. Combined time-series resistivity and geochemical tracer techniques to examine submarine groundwater discharge at Dor Beach, Israel. *Geophys. Res. Lett*. **2006a**, 33, L24405, doi:10.1029/2006GL028282.

(22) Cable, J.E.; Burnett, W.C.; Chanton, J.P.; Corbett, D.R.; Cable, P.H. Field evaluation of seepage meters in the coastal marine environment. *Estuar, Coast Shelf Sci,* **1997**, 45, 367-375.

(23) Burnett, W.C.; Dulaiova, H. Estimating the dynamics of groundwater input into the coastal zone via continuous radon-222 measurements. *J. Environ. Radioact.* **2003**, 69, 21-35.

(24) Dulaiova, H.; Peterson, R.; Burnett, W.C.; Lane-Smith, D. A multi-detector continuous monitor for assessment of 222Rn in the coastal ocean. *J. Radioanal. Nucl. Chem.* **2005**, 263, 361-365.

(25) Moore W.S. Radium isotopes as tracers of submarine groundwater discharge in Sicily. *Cont. Shelf Res.* **2006**, 26, 852-861.

(26) Swarzenski, P.W.; Orem, W.G.; McPherson, B.F.; Baskaran, M.; Wan, Y. Biogeochemical transport in the Loxahatchee river estuary: The role of submarine groundwater discharge. *Mar. Chem.* **2006b**, 101, 248-265.

(27) Swarzenski, P.W.; Reich, C.; Kroeger, K.; Baskaran, M. Ra and Rn isotopes as natural tracers of submarine groundwater discharge in Tampa Bay, FL. *Mar. Chem.* **2007**, 104, 69-84.

(28) Urish, D.W.; Frohlich, R.K. Surface electrical resistivity in coastal groundwater exploration. *Geoexploration* **1990**, 26, 267-289.

(29) Moore, W.S.; Arnold, R. Measurements of ^{223}Ra and ^{224}Ra in coastal waters using a delayed coincidence counter. *J. Geophys. Res.* 1996, 101, 1321-1329.

(30) Day-Lewis, F.D.; White, E.A.; Belaval, M.; Johnson, C.D.; Lane, J.W. Continuous resistivity profiling to delineate submarine ground-water discharge - examples and limitations. *Leading Edge* **2006**, 25, 724-728.

(31) Swarzenski, P.W.; Charette, M.; Langevin, C. *An autonomous, electromagnetic seepage meter to study coastal groundwater / surface water exchange;* U.S. Geological Survey; Open-File Report 2004-1369; 2004.

(32) Martens, C.S.; Kipphut, G.W.; Klump, J.V. Sediment-water chemical exchange in the coastal zone traced by in situ radon-222 flux measurements. *Science* **1980**, 208, 285-288.

(33) Dulaiova, H.; Burnett, W.C.; Chanton, J.P.; Moore, W.S.; Bokuniewicz, H.J.; Charette, M.A.; Sholkovitz, E. Assessment of groundwater discharges into West Neck Bay, New York, via natural tracers. *Cont. Shelf Res.* **2006**, 26, 1971-1983.

(34) Robinson, C.; Li, L.; Barry, D.A. Effect of tidal forcing on a subterranean estuary. *Adv. Water Resour.* **2006**, doi:10.1016/j.advwatres.2006.07.006.

(35) Burnett, W.C.; Santos, I.; Weinstein, Y.; Swarzenski, P.W.; Herut, B. Remaining uncertainties in the use of Rn-222 as a quantitative tracer of submarine groundwater discharge. In: *A New Focus on Groundwater-Seawater Interactions*; International Association of Hydrological Sciences (IAHS); Special Volume; 2007; pp 1-12.

(36) Paulson, A.J.; Curl, Jr., H.C.; Feely, R.A. The biogeochemistry of nutrients and trace metals in Hood Canal, a Puget Sound fjord. *Mar. Chem.* **1993**, 43, 157-173.

(37) Paulson, A.J.; Konrad, C.P.; Frans, L.M.; Noble, M.; Kendall, C.; Josberger, E.G.; Huffman, R.L.; Olsen, T.D. *Freshwater and saline loads of dissolved inorganic nitrogen to Hood Canal and Lynch Cove, Western Washington;* U.S. Geological Survey; Scientific Investigations Report 2006-5106; 2006.

(38) Capone, D.G.; Zehr, J.P.; Paerl, H.W.; Bergman, B.; Carpenter, E.J. Trichodesmium, a globally significant marine cyanobacterium. *Science* **1997**, 276, 1221-1229.

(39) Capone, D.G.; Knapp, A.N. A marine nitrogen cycle fix? *Nature* **2007**, 445: 159-160.

(40) Wiegner, T.N.; Seitzinger, S.P. Bioavailability of dissolved organic carbon and nitrogen from pristine and polluted freshwater wetlands. *Limnol. Oceanogr.* **2004**, 49, 1703-1712.

Table 1. A time series of groundwater, surface water, and low tide seep water salinity and nutrient data (μM) collected at the Merrimont site on 06/07/2006. Low tide occurred at ~09:00; high tide at ~01:00.

			salinity	NH_4	Si	PO_4	NO_3+NO_2	DIN	DON	TDN
				μM						
Piezo[a]	1	9:45	14.6	0.1	157.0	0.5	19.8	19.9	6.3	26.1
	2	10:45	17.6	0.1	146.0	0.7	19.2	19.3	6.9	26.1
	3	11:45	14.7	0.0	151.0	0.9	20.5	20.5	5.0	25.5
	4	12:45	14.5	0.0	157.0	0.8	21.1	21.1	5.3	26.4
	5	13:45	15.5	0.0	145.0	1.3	23.7	23.7	3.6	27.3
	6	14:45	16.8	0.0	149.0	0.7	27.1	27.1	3.8	30.9
	7	15:45	17.3	0.0	137.0	1.3	28.9	28.9	4.4	33.3
	8	16:45	18.1	0.0	134.0	1.3	30.2	30.2	4.3	34.5
	9	17:45	17.1	0.0	145.0	1.5	26.3	26.3	6.4	32.7
	10	18:45	17.1	0.0	137.0	1.6	24.7	24.7	5.9	30.6
		mean	16.3	0.0	145.8	1.1	24.2	24.2	5.2	29.4
		±	1.4	0.0	8.1	0.4	3.9	3.9	1.1	3.4
Surface water[b] **(dock)**	1	9:45	25.3	0.5	62.8	1.0	1.4	1.8	16.3	18.1
	2	10:45	24.6	1.3	61.2	1.7	1.2	2.5	7.9	10.3
	3	11:45	25.1	0.7	159.0	3.8	0.7	1.4	8.4	9.7
	4	12:45	25.8	1.6	81.3	2.0	0.7	2.3	12.6	15.0
	5	13:45	26.7	1.4	62.2	0.7	0.2	1.6	9.7	11.3
	6	14:45	25.9	0.6	56.2	1.0	0.1	0.7	11.1	11.8

	7	15:45	26.0	0.3	52.7	0.9	0.0	0.3	10.6	11.0
	8	16:45	26.6	0.3	53.8	1.0	0.2	0.5	7.8	8.3
	9	17:45	26.7	0.1	55.5	1.0	1.2	1.3	10.5	11.7
	10	18:45	26.5	0.6	62.7	1.1	2.2	2.8	8.1	10.9
		mean	25.9	0.7	70.7	1.4	0.8	1.5	10.3	11.8
		±	0.7	0.5	32.1	0.9	0.7	0.8	2.7	2.8
Seep water[c]		10:00	4.6	0.1	170.0	4.3	6.8	6.8	7.7	14.6

[a] Collected using a drive-point piezometer from an equilibrated horizon 185cm below mean sea level off the Merrimont dock at the high tide line.

[b] Collected at the seaward end of the dock with a peristaltic pump.

[c] Collected at the low tide water line, close to the seaward end of the dock (June 11, 2006).

Table 2. Radium, ^{228}Th and radon activities in groundwater ('Piezo') and surface water samples at the Merrimont dock site (06/07-10/2006). For geographic locations of the Lynch Cove surface water column (HC) and Skokomish River (SR1) sites, see Figure 1. Expected error for ^{223,224}Ra is ~10%.

	salinity	^{226}Ra	^{228}Ra	^{223}Ra	^{224}Ra	^{222}Rn
		dpm 100L^{-1}				dpm L^{-1}
Piezo-1[a,b,c]	14.6	8.1 ± 1.2	25.5 ± 2.9	3.0	44.3	158 ± 11
Piezo-5	17.3	8.8 ± 1.2	34.0 ± 3.0	2.6	87.9	129 ± 25
Piezo-10	17.1	6.6 ± 1.1	5.1 ± 1.9	2.2	97.2	140 ± 35
Surface-1[b,c]	25.1	5.0 ± 0.4	1.7 ± 0.3	0.1	1.1	n/m
Surface-5	25.9	4.6 ± 0.4	3.0 ± 0.5	0.1	1.0	n/m
Surface-10	26.7	5.4 ± 0.4	1.1 ± 0.4	0.1	1.5	n/m
HC1[c]	24.4	2.9 ± 0.3	1.9 ± 0.5	0.0	0.8	n/m
HC2	23.5	3.2 ± 0.3	2.1 ± 0.4	0.0	1.0	n/m
HC3	24.8	3.8 ± 0.3	1.9 ± 0.5	0.2	0.6	n/m
HC4	24.3	3.8 ± 0.3	1.6 ± 0.5	0.2	1.0	n/m
HC5	21.5	5.9 ± 0.3	4.7 ± 0.5	0.3	10.2	n/m
Skokomish River[c,d]	0.01	0.4 ± 0.1	0.0 0.0	0.1	0.2	n/m

[a] Collected using a drive-point piezometer from an equilibrated horizon 185cm below the seafloor at the high tide line by the Merrimont dock.

[b] Numbering sequence and associated attributes in 'Piezo' and 'Surface' samples match those presented in Table 1.

[c] All Ra samples were collected by filtering water directly through pre-weighed Mn-O2 cartridges with a peristaltic pump. Surface, HC and the Skokomish samples were pumped from 0.5m water column depth.

[d] Collected from the SR 106 bridge (see Figure 1 for location).

n/m Not measured.

Table 3. Absolute nutrient loading estimates (mol d^{-1}) into Lynch Cove derived using time series ^{222}Rn, and excess ^{226}Ra SGD rates. Results are compared to previous nutrient loading estimates. Cumulative uncertainty is estimated at ~25%, based on endmember concentrations.

Approach	SGD	NH_4	Si	PO_4	NO_3+NO_2	DIN	DON	TDN
	$m^3 s^{-1}$	mol d^{-1}						
Rn[a]	28	28	3.6×10^5	2.6×10^3	5.9×10^4	5.9×10^4	1.3×10^4	7.2×10^4
Ra[b]	24 (86%)[c]	24	3.0×10^5	2.2×10^3	5.0×10^4	5.0×10^4	1.1×10^4	6.0×10^4
Seep water[d]	28	240	4.2×10^5	1.1×10^4	1.7×10^4	1.7×10^4	1.9×10^4	3.6×10^4
Manual seepmeter[e]	3.4	28	5.0×10^4	1.3×10^3	2.0×10^3	2.0×10^3	2.3×10^3	4.3×10^3
Mass balance[f]	1.2[d]	--	--	--	--	4.2×10^3	--	--
Rivers/ Streams[g]	--	--	--	--	--	2.1×10^3	--	--
Atmospheric Deposition[g]	--	--	--	--	--	3.3×10^2	--	--

[a] Rn-derived SGD rate (total; saline + fresh water contribution) at Merrimont dock (SGD-scaled area = 2.89×10^6 m^2). Mean groundwater nutrient concentrations from Table 1.

[b] Ra-derived SGD rate (saline contribution) for Lynch Cove (area = 2.7×10^7 m^2). Mean groundwater nutrient concentrations from Table 1.

[c] Ratio (%) of saline (Ra-derived) : total (Rn derived) SGD.

[d] Nutrient loading estimates calculated using nutrient concentrations of low-tide seep water (Table 1) and Rn-derived SGD rates. (SGD-scaled area = 2.89 x 10^6 m^2).

[e] Nutrient loading estimate based on mean manual seepage meter-derived SGD rates and seep-water nutrient concentrations from Table 1. (SGD-scaled area = 2.89 x 10^6 m^2).

[f] Mass balance-based DIN loading estimate using a mean fresh groundwater DIN concentration of 43.6 μM (37).

[g] Data (September and October 2004) from Paulson et al. (37).

Figure captions

Figure 1. Study site map of Lynch Cove, the terminus of Hood Canal, a fjord-like western extension of Puget Sound, WA. Inset map shows time-series location at Merrimont. HC and SR1 designate ^{224,223,} ^{228,226}Ra surface (z = -0.5m) water sampling sites in Lynch Cove/Hood Canal and the Skokomish River, respectively. Piezometer location near the high tide line, ~10m west of the walkway to the floating dock.

Figure 2. Stationary, time-series, multi-electrode resistivity profiles across a beach face at the Merrimont site as a function of water level. Inversion parameters were held constant for each time step. The resistivity cable consisted of 56 electrodes, spaced 2m apart and routed into an 8-channel receiver (AGI SuperSting R8 Marine) through an external switching box. To highlight subsurface resistivity change at the land / sea interface, images reflect only the first 40m of data. Inset graph of water level data collected from a Solinist Diver midway down cable, at electrode 28. Electrode positions reflect actual bathymetry.

Figure 3. Five-day time series at the Merrimont site of (A) bottom water ^{222}Rn activities (dpm L^{-1}), (B) bidirectional electromagnetic (EM) seepage meter results (cm d^{-1}); the zero discharge line is shown for reference, and (C) bottom water conductivities (mS cm^{-1}) collected from the top of a EM seepage meter dome. The reference line in (C) denotes the mean conductivity (40.7 mS cm^{-1}) of the bottom waters. Water level data in (A) was collected from the same Solinist Diver mounted on the seepage meter dome. At low tide,

there was ~0.2m of water above the seepage meter and the time-series Rn intake. The seepage meter and the Rn intake line were located just off the seaward side of the dock.

Figure 4. Dissolved inorganic nitrogen (DIN) as a function of PO_4^{-3} in groundwater and surface water samples. The 16:1 Redfield ratio line is shown for reference.

Figure 5. Molar ratio of A) DIN/PO_4^{-3} and B) percent DON/TDN from groundwater ('gw'; n = 10), surface water ('sw'; n=10) and one low tide seep water ('seep') sample.

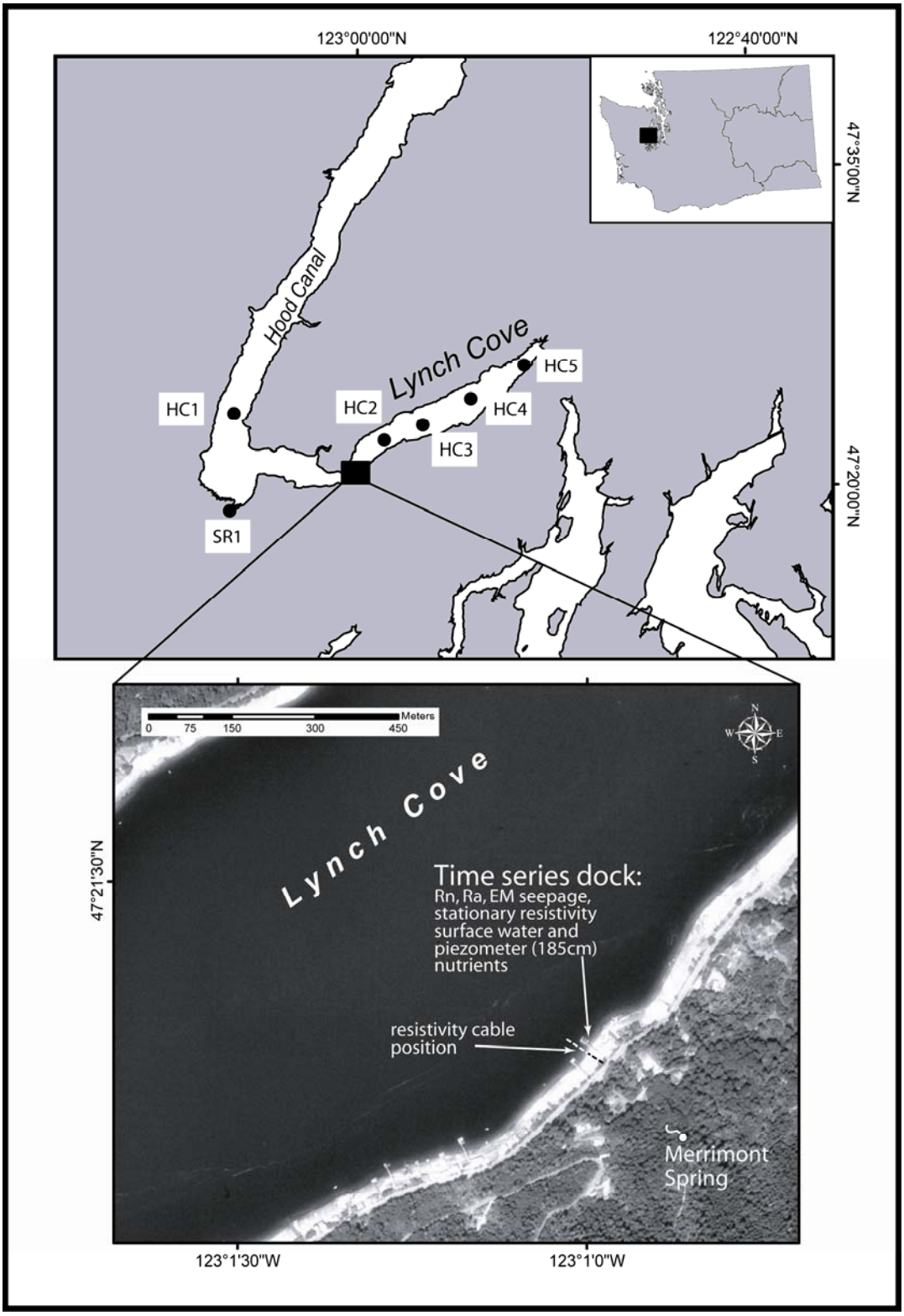
123°00'00"N
122°40'00"N
47°35'00"N
47°20'00"N
Hood Canal
Lynch Cove
HC1
HC2
HC3
HC4
HC5
SR1
Meters
0 75 150 300 450
N
W
E
S
Lynch Cove
47°21'30"N
Time series dock:
Rn, Ra, EM seepage,
stationary resistivity
surface water and
piezometer (185cm)
nutrients
resistivity cable
position
Merrimont
Spring
123°1'30"W
123°1'0"W

Figure 1.

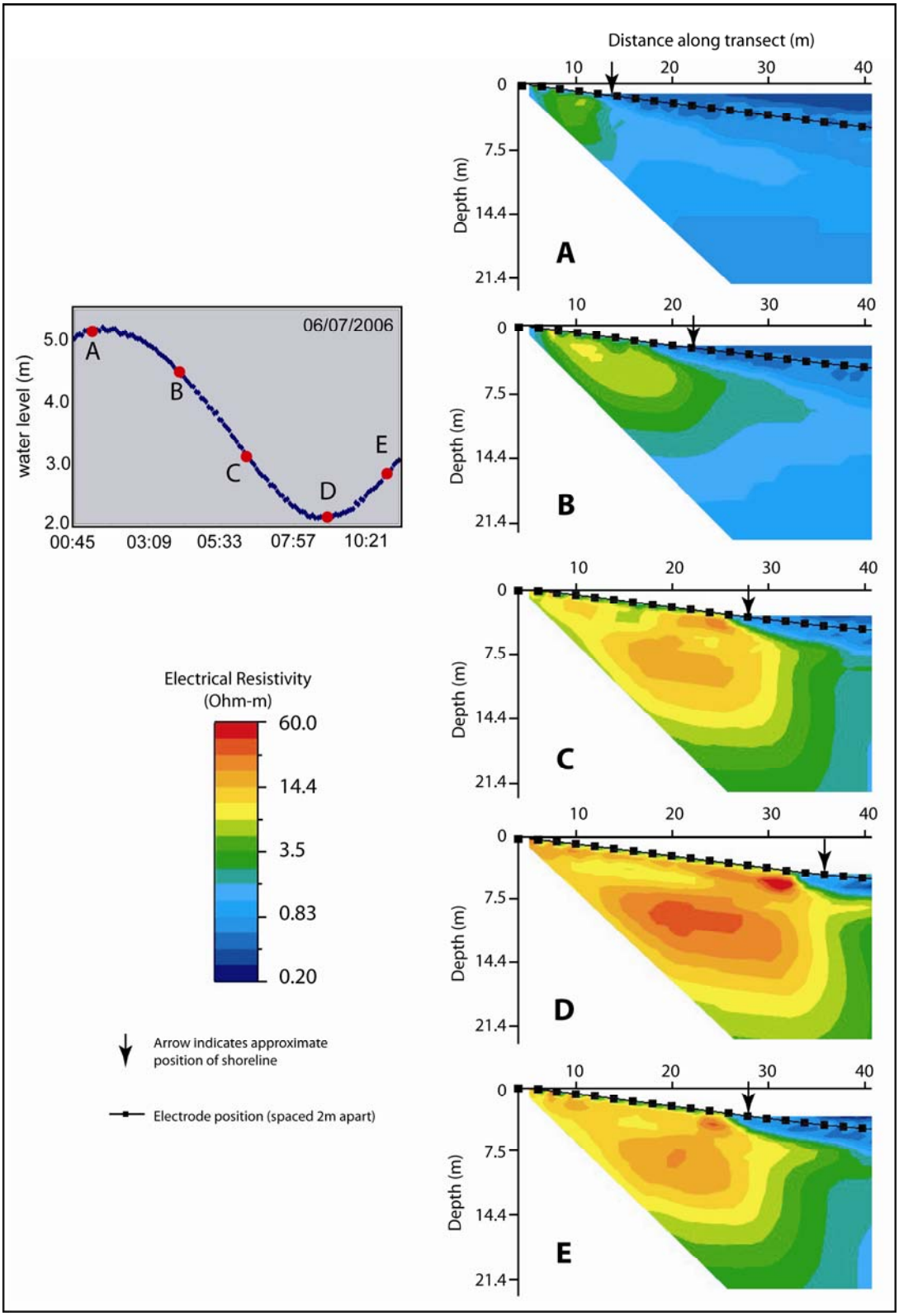
Distance along transect (m)
10
20
30
40
0
7.5
14.4
21.4
Depth (m)
A
B
C
D
E
06/07/2006
water level (m)
5.0
4.0
3.0
2.0
00:45
03:09
05:33
07:57
10:21
Electrical Resistivity
(Ohm-m)
60.0
14.4
3.5
0.83
0.20
Arrow indicates approximate position of shoreline
Electrode position (spaced 2m apart)

Figure 2.

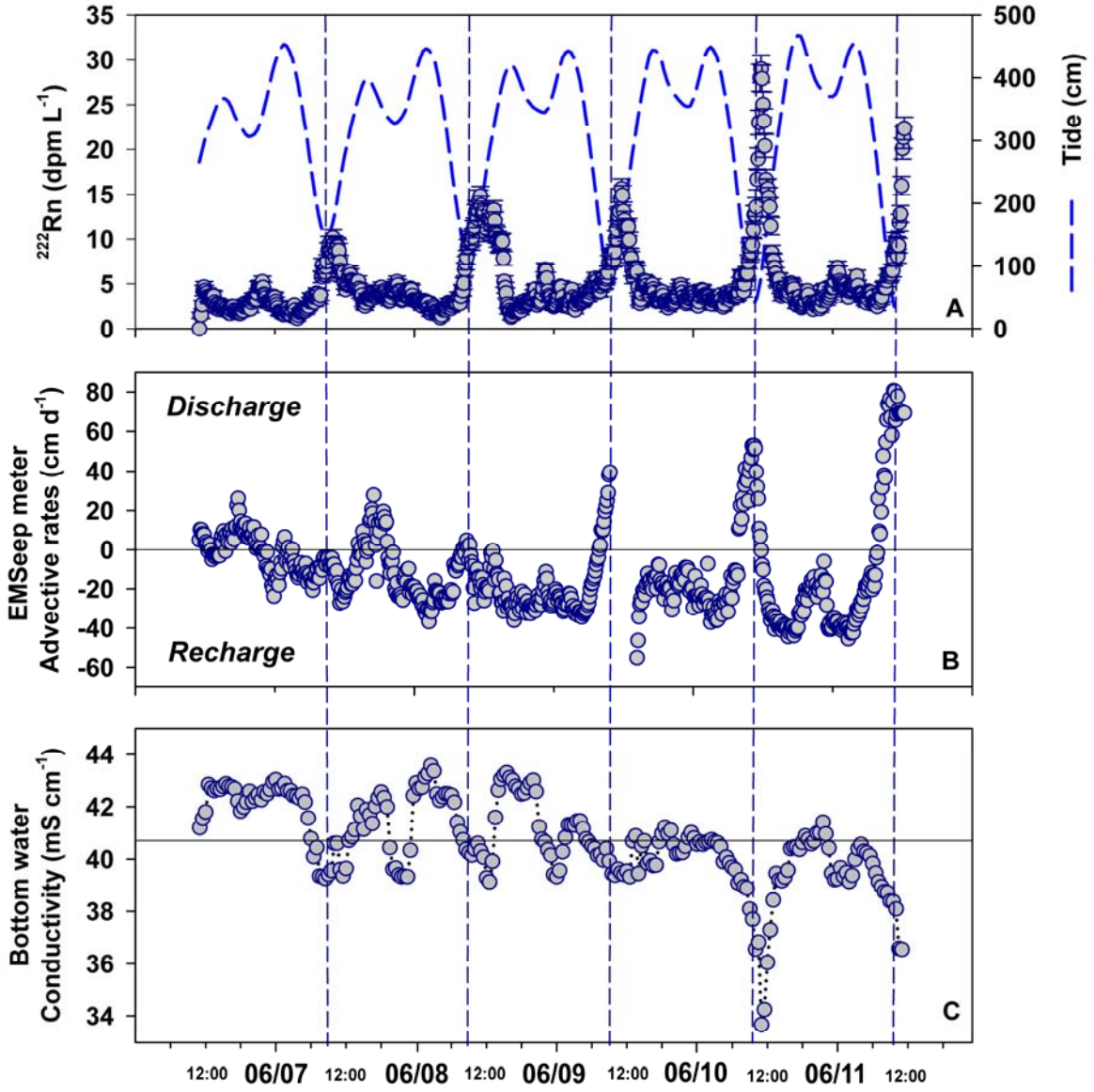
222Rn (dpm L-1)
Tide (cm)
A
Discharge
Recharge
EMSeep meter
Advective rates (cm d-1)
B
Bottom water
Conductivity (mS cm-1)
C
12:00
06/07
06/08
06/09
06/10
06/11

Figure 3.

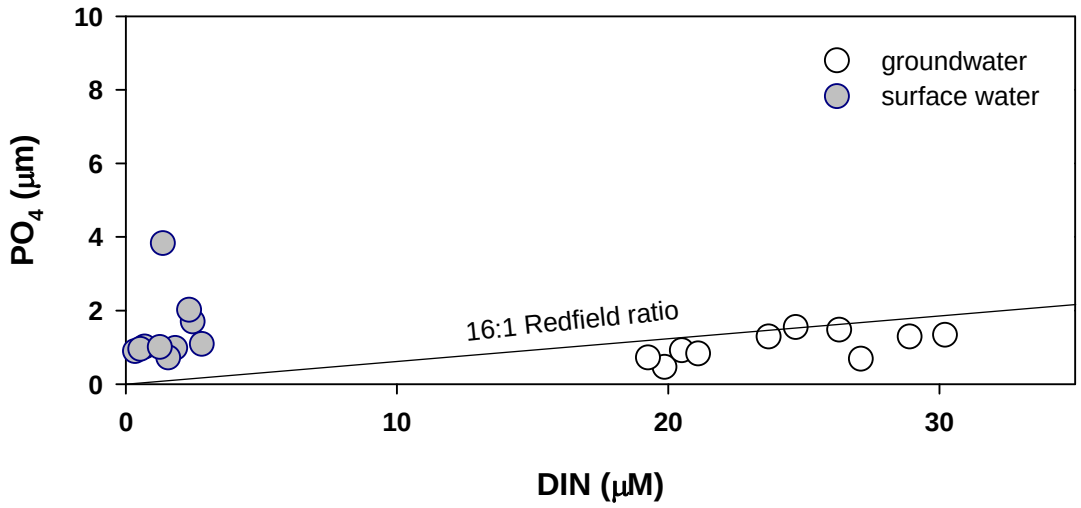
10
8
6
4
2
0
PO4 (μm)
0
10
20
30
DIN (μM)
groundwater
surface water
16:1 Redfield ratio

Figure 4.

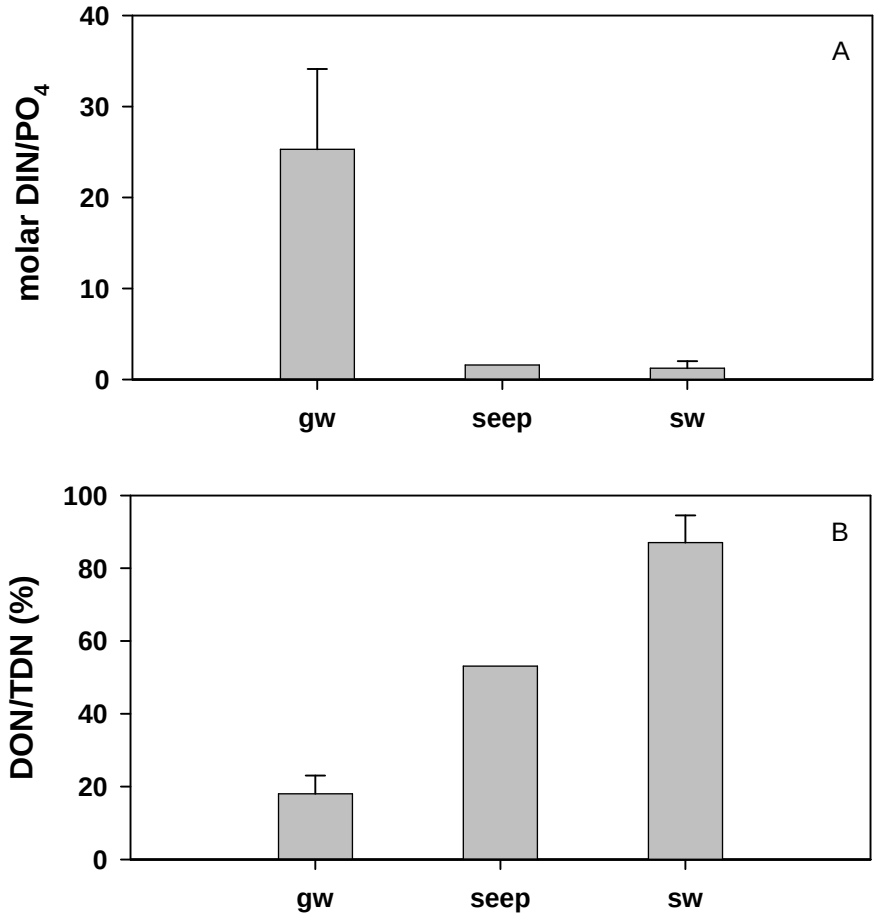
A
molar DIN/PO4
40
30
20
10
0
gw
seep
sw
B
DON/TDN (%)
100
80
60
40
20
0
gw
seep
sw

Figure 5.